P5.41 IMAGERY INTERPRETATION OF MICROWAVE OBSERVATIONS BY AMSU AND TMI OVER A COMPLEX TROPICAL REGION

Benjamin Ruston*, Thomas H. Vonder Haar, and John Forsythe
Center for Geosciences / Atmospheric Research at the Department of Atmospheric Science at Colorado State University, Fort Collins, Colorado

1. INTRODUCTION

Satellite microwave radiometers have been used for over thirty years to observe the earth and derive atmospheric parameters. The number of meteorological satellites in orbit with microwave capabilities continues to increase, with new satellites featuring better spatial resolution, and wider spectral range. From the new array of radiometers, an age with multiple calibration procedures is becoming possible, and an effective microwave radiance shell surrounding the Earth can be constructed. A simple first step towards this goal is to compare co-temporal observations from the AMSU and TMI instruments, which provide over 25 channels of various frequencies and polarizations. In this study, we present current theory and technique to interpret microwave imagery over the Malaysian-Indonesian region, emphasizing utility to forecasting. The area has widely varying features including mountain terrain, rain forest, swampland, lakes, and surrounding ocean. We demonstrate and discuss how physical parameters such as soil moisture, precipitation, cloud liquid water, and total column water vapor create differences in brightness temperatures across the microwave spectrum.

Microwave radiometers on weather satellites currently span the frequency range of 10 - 183 GHz. The resolution of microwave radiometers is diffraction limited, meaning that lower frequency observations require a larger physical antenna to have the same ground resolution as higher frequency observations. However, lower frequency microwave data has advantages because the atmosphere is more transparent, allowing better remote sensing of the surface.

When examining microwave imagery additional considerations should include knowledge of the terrain being evaluated, and resolution of the instrument being used. The difference in soil moisture between a desert, and a river basin creates noticeable differences in lower frequencies. Detailed maps including topography are useful because of temperature gradients due to terrain height. Lower instrument resolution will begin to average affects of clouds, or surface features such as small bodies of water. Keeping these non-atmospheric affects in mind, we begin to explore atmospheric affects due to gases (oxygen and water vapor), and liquid and ice water.

* *Corresponding author address:* Benjamin Ruston, CSU, Dept. of Atmos. Science, Ft. Collins, CO 80523 Ruston@cira.colostate.edu

2. EMISSION CHARACTERISTICS

Interpretation of microwave imagery begins with an examination of the sources of the radiation. Microwave radiation reaching space from the Earth-atmosphere system is a combination of emission and scattering. Emitters in the 10 to 183 GHz range include the land and ocean surface, water vapor, water and ice clouds, and precipitation. Scattering occurs at the land and ocean surface, and in clouds. Thin ice clouds composed of small ice crystals (e.g. cirrus) are essentially transparent in the microwave, especially at frequencies below 50 GHz. The fact that microwave remote sensing and atmospheric retrievals can be performed in the presence of clouds is a driving force behind satellite microwave radiometry. Microwave data can also retrieve parameters not typically sensed with visible or infrared data, such as sea surface wind speed. Microwave radiometers can also be built with low noise values. These three features, ability to perform in clouds, ability to retrieve unique environmental parameters, and stable calibration ensure that satellite microwave remote sensing will play and larger and increasingly important role in atmospheric science.

2.1 Surface

By definition, a blackbody has a uniform emission efficiency (emissivity) of one throughout all frequencies. No body on Earth is a perfect blackbody and as a consequence the variation of emissivity with frequency is a property utilized in microwave imagery interpretation. When a body has an emissivity of one the temperature derived from the radiance will correspond to the temperature of the body. However, an emissivity of 0.5 will make a body at 300 K radiate like a blackbody of 150 K. Dry land has a high emissivity, often greater than 0.9, while increasing soil moisture or a moist canopy of vegetation will drive the emissivity of the surface down. For example, at low (< 30GHz) frequencies a desert has a much greater emissivity than swampland, so even if the surface temperatures are identical, microwave brightness temperatures will show the desert as warmer than the swampland. The emissivity of land is greatly variable at a single frequency, with the greatest differences at frequencies of 10 - 30 GHz, which are used to detect soil moisture, or infer properties of the vegetative canopy (Schmugge, 1985). Many parameters such as dew, rainfall, vegetation type, soil type, and urbanization effects affect land emissivity over the globe. As a consequence land surfaces exhibit highly temporally and spatially variant emissivity patterns.

Ocean emissivity is not highly variable at a single frequency, with temperature, salinity, and wind speed determining the emission. Lower microwave frequencies are used to find sea surface temperature (Stogryn, 1967), and wind speed (Williams, 1969; Hollinger, 1971; and Webster et al., 1976). The ocean emissivity also varies steadily over frequency; at lower frequencies (< 20 GHz) the ocean's emissivity is about 0.4 and increases with increasing frequency. This large discrepancy in emissivity at low frequencies causes a difference in radiance over ocean and land, allowing for easy land detection.

Polarization is of paramount importance in microwave remote sensing, unlike visible and infrared measurements. The sea surface is highly polarized, while land surfaces exhibit low polarization, with some exceptions like desert sand and ice. Atmospheric effects case the outgoing radiation to space to become less polarized. Atmospheric retrievals exploit this change in the polarizations signal. Vertical and horizontal polarization measurements are typically sufficient to retrieve a wide range of phenomena. Fully polarimetric (Stokes) vector measurements may be required to sense sea surface wind direction (Yueh, S. H., 1997). For a microwave instrument without a constant viewing angle, such as the cross-track scanning AMSU, each field of view has a mixture of vertical and horizontal polarizations. This is benefit of a conical scanning instrument. The incident angle is constant which simplifies surface effects. Measurements from any field of view in a conical instrument can be combined to create composites of features like surface emissivity (Jones and Vonder Haar, 1997). Such compositing is not easily accomplished with a cross-track instrument.

2.2 Atmosphere and Clouds

The atmosphere's gaseous extinction increases with frequency in the microwave regime due to the water vapor continuum. Superimposed over this gradual increase are strong absorption bands due to water vapor, and oxygen. In a clear atmosphere, the absorption and reemission by these gases can be detected.

To examine the effect of cloud liquid water and ice, we used the Goddard Cumulus Ensemble (GCE) model created at Goddard Space Flight Center (Tao and Simpson, 1993). Brightness temperatures were derived from the cloud profiles taken from this model using a plane parallel radiative transfer model with the Eddington approximation and explicit Mie calculations (Kummerow, 1993). The underlying surface was a specular ocean surface with a temperature of 300 K, with the emissivity calculation following the models of Stogryn (1967) and Hollinger (1971). We have prepared five cases of varying properties: a clear sky case, a non-precipitating cloud, two precipitating clouds of varying precipitation rates, and finally a cloud with little rain and a high ice content. These five cases are presented in Figure 1, and a synopsis of their properties in Table 1.

TABLE 1

CASE	Surface Rain Rate (mm/hr)	Column Water Vapor (mm)	Column Precip Liq + Cld Water (mm)	Column Precip Ice + Cld Ice (mm)
Clear	0.000	67.693	0.000	0.000
No Rain Cld	0.000	71.570	1.180	0.000
Lt Rain	1.148	71.481	2.108	0.000
Hvy Rain	19.347	74.821	2.017	1.162
Ice Cld	0.214	67.746	1.380	2.831

In general, the presence of clouds and rainfall obscure the gaseous absorption peaks. Three regimes across the frequency range can be loosely defined, liquid water emission, ice scattering, and a third regime where liquid water emission and ice scattering compete. The first regime is from 10 GHz to the water vapor band at 22 GHz. Emission by liquid water warms the brightness temperatures above the cold ocean surface. As more and larger raindrops are found the warming at lower frequencies increases more dramatically. The non-precipitating cloud had much higher low-level water vapor than the clear or ice cloud case and displayed a warmer background due to the vapor emission.

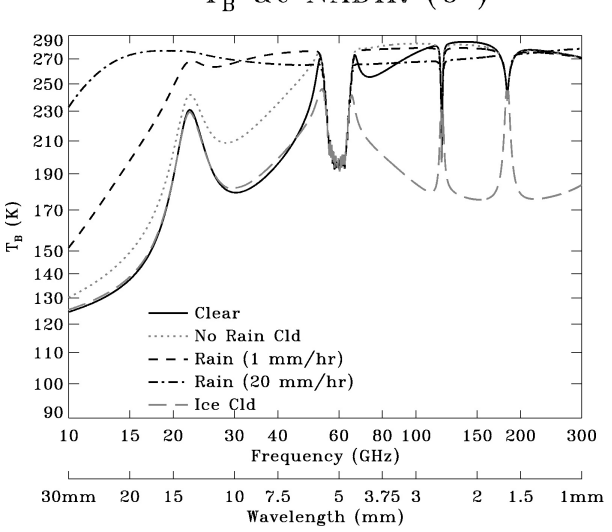

FIGURE 1: Profile of brightness temperature with respect to frequency for five cases. Vertical cloud profiles are from the Goddard Cumulus Ensemble model.

Between the water vapor absorption peak at 22 GHz and the oxygen band and around 60 GHz the liquid water emission, and ice scattering begin to compete. This is displayed well in the two precipitating cloud cases where, the brightness temperature profile for the heavily raining case begin to grow cooler than the lightly raining case, due to the scattering by precipitation size ice. Also notice the ice cloud begins to drop below the clear sky case.

At frequencies greater than 80 GHz precipitation-size ice increases scattering and dominates the

brightness temperature. For the two precipitating cloud cases notice though the heavily raining case is colder than the lightly raining by around 30 GHz it doesn't grow colder than the ocean background until above 80 GHz. With the largest scattering signature found in the ice cloud which strongly depresses the brightness temperature. At the center of the large oxygen absorption band around 60 GHz; all cases have the same brightness temperature, because this portion of the spectrum is sensitive to the upper levels of the atmosphere. However, in the wings of this absorption band the band brightness temperature come from lower in the atmosphere until enough liquid water makes the atmosphere sufficiently opaque.

3. IMAGERY INTERPRETATION

On September 13, 1999 the TRMM Microwave Imager (TMI) and Advanced Microwave Sounding Unit (AMSU) instruments both had descending passes over the Indonesian region of Borneo and Celebes within minutes of each other. The TMI instrument is a conical scanner, at a constant scan angle of 53° allowing for polarized channels. Imagery from four channels in TMI was chosen for presentation, the 10.65V, 19.35H, 37.0H, and 85.5V GHz. Two sounding channels were selected from the AMSU instruments, centered at 50.3 GHz and 183.3±7 GHz. Infrared imagery at 10.8 μm from both the Visible Infrared Scanner (VIRS) and the Advanced Very High Resolution Radiometer (AVHRR) is also presented. From this selection of channels we can make determinations about the land and ocean boundaries, see resolution issues between channels and satellites, and determine objectively some surface features, heavily raining clouds, and clouds with large column ice content. This provides a good example of issues encountered by a real-time user of microwave imagery, such as a forecaster.

TABLE 2

Channel Frequency (GHz)	**EFOV** (km)	**NEΔT** (K)
10.65V	63 × 37	0.63
19.35H	30 × 18	0.47
37.0H	16 × 9	0.31
50.3	48 × 48 (1.9°) 79 × 148 (57.6°)	0.219
85.5V	7 × 5	0.52
183.3±7	16 × 16 (0.6°) 27 × 53 (59.2°)	0.60

The imagery resolution in both the AMSU and TMI instruments increases with increasing frequency (see Table 2). This is demonstrated by the fuzzy edges seen around the islands and clouds at 10.65V GHz, which can be contrasted with the well-defined land edges at 85.5V GHz. The infrared channel on AVHRR has a 1 km resolution at nadir and corresponds to ~28,000 GHz. The draw back however to the greater resolution in the infrared is that the emissivity differences are lost.

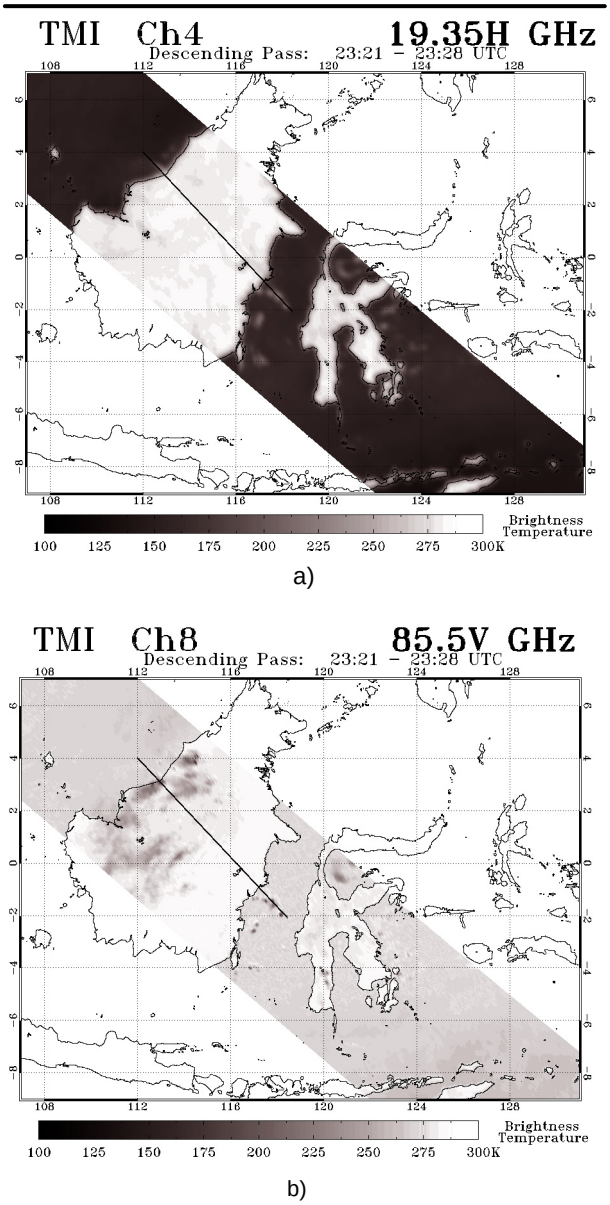

FIGURE 2: Images from the TRMM microwave imager (TMI) at two frequencies: a) 19.35H and b) 85.5V GHz.

In the two lower frequency channels on the TMI at 19.35H and 10.65V GHz, the land-ocean contrast is a dominant feature. The land surface variations reveal swampland around the small lakes at 112E and 116E in Borneo and identification of river basins is possible as well. These two swampland regions have lower brightness temperatures due to the lower emissivity of the land surface. The emissivity change is due to soil moisture content, and vegetation. Channels at 19.35H and 10.65V GHz cannot easily distinguish clouds over

land, unless extremely large raindrops are present. Over ocean however clouds are more easily detected due to the cold ocean background. These channels are sensitive again to the larger precipitation size particles. The 19.35H GHz channel has increased sensitivity to water vapor not present in the lower frequency channel. The clouds that are apparent in both the 19.35H, and the 10.65V channel have very large water drops, and are precipitating heavily. Those that are present in only the 19.35 GHz may be thicker clouds with smaller precipitation particles. There may be heavy rain on the sub-pixel scale that is undetected due to the sensor resolution (refer to Table 2); this is referred to as the beam-filling problem (Kummerow and Giglio, 1994). Examining the cloud field in both the infrared images and in these two microwave channels gives an idea of which clouds, over the ocean, are precipitating heavily.

The two TMI channels centered at 37.0H and 85.5V GHz begin to give highly resolved cloud boundaries over both ocean and land, and are both referred to as imaging channels due to relative minima in the extinction due to the water vapor continuum. At these frequencies the total column water vapor is extremely important. In the tropics the high column water vapor dominates the signal, and these channels become sensitive to changes in this total. While in a polar scene with low column water vapor the channels become sensitive to liquid water (Petty, 1992). In our scene the 37.0H GHz channel has a greater contribution due to liquid water, while the 85.5V GHz channel is still dominated by the water vapor emission and sensitivity to liquid water is small. Where precipitation size ice exists the radiation at 85.5V GHz is scattered by these particles. This scattering reduces the radiance at the satellite sensor and creates lower brightness temperatures. Over land, radiation at 85.5V GHz frequency is due to scattered surface radiation, while over the ocean the scattered radiation is due to water vapor and liquid water emission. The sensitivity to ice scattering makes the 85.5V GHz channel very useful for detecting precipitation size ice.

In summary, the variation of brightness temperature across the microwave spectrum allows interpretive analysis of the land surface (swampland and river basin identification). Clouds appear quite differently through the microwave spectrum with large liquid precipitation particles warming the lower frequencies, and precipitation-size ice scattering, and dominating by 80 GHz. Images using color enhancements can emphasize the land surface brightness temperature variation, atmospheric liquid emission, and ice scattering. These images can be used to make real-time determinations about areas of precipitation, intensity of precipitation, and amount of precipitation size ice.

(on-line at: http://cassiopeia.cira.colostate.edu/AMS2001/)

4. ACKNOWLEDGEMENTS

We appreciate the assistance of Dr. Christian Kummerow, Stan Kidder, and Andy Jones who provided technical assistance and suggestions.

This research, conducted at CIRA/CSU, has been supported by the United States Department of Defense Center for Geosciences / Atmospheric Research, Cooperative Agreement DAAL01-98-2-0078. We also acknowledge partial support from the Ball CMIS team via STC-METSAT.

5. REFERENCES

Hollinger, J. P., 1971: Passive Microwave Measurements of Sea Surface Roughness. *IEEE Trans. Geosci. Electron., GE-9,* pp. 169.

Jones, A. S., and T. H. Vonder Haar, 1997: Microwave Surface Emittance Over Land Using Coincident Microwave and Infrared Satellite Measurements. *Journal of Geophysical Research*, **102**, D12, 13609-13626.

Kidder, S. Q., and Vonder Haar, T. H., 1995: Satellite Meteorology: An Introduction. *Academic Press*, San Diego.

Kummerow, C., and L. Giglio, 1994: A Passive Microwave Technique for Estimating Rainfall and Vertical Structure Information from Space. Part I: Algorithm Description. *Journal of Applied Meteorology*, **33**, 1, pp. 3 - 18.

Kummerow, C., 1993: On the Accuracy of the Eddington Approximation for Radiative Transfer in the Microwave Frequencies. *Journal of Geophysical Research*, **98**, D2, pp. 2757-2765.

Petty, G. W., Katsaros, K. B., 1992: The Response of the SSM/I to the Marine Environment. Part I: An Analytic Model for the Atmospheric Component of Observed Brightness Temperatures. *Journal of Atmospheric and Oceanic Technology*, **9**, 6, pp. 746 - 761.

Prigent, C., Rossow, W. B., and E. Matthews, 1997: Microwave Land Surface Emissivities estimated from SSM/I Observations. *Journal of Geophysical Research*, **102**, D18, pp.21867-21890.

Schmugge, T., 1985: Remote Sensing of Soil Moisture. *Hydrological Forecasting*. John Wiley & Sons Ltd., Chichester, pp. 101 - 124.

Stogryn, A., 1967: The Apparent Temperature of the Sea at Microwave Frequencies. *IEEE Transactions on Antennas and Propagation*, **AP-15**, 2, pp. 278-286.

Tao, W.-K., and J. Simpson, 1993: The Goddard Cumulus Ensemble Model. Part I: Model Description. Terrestrial. *Atmospheric Oceanic Sciences,* 4, pp. 35-72.

Webster, W. J., Wilheit, T. T., Ross, D. B, and P. Gloersen, 1976: Spectral Characteristics of the Microwave Emission From a Wind-Driven Foam-Covered Sea. *Journal of Geophysical Research*, **81**, 18, pp. 3095-3099.

Williams, G. F., 1969: Microwave Radiometry of the Ocean and the Possibility of Marine Wind Velocity Determination from Satellite Observations. *Journal of Geophysical Research*, **74**, 18, pp. 4591-4594.

Yueh, Simon H., 1997: Modeling of Wind Direction Signals in Polarimetric Sea Surface Brightness Temperatures. *IEEE Transaction on Geoscience and Remote Sensing*, **35**, 6, pp. 1400 - 1418.